

Deformations in Si–Li Anodes Upon Electrochemical Alloying in Nano-Confined Space

Benjamin Hertzberg,[†] Alexander Alexeev,[‡] and Gleb Yushin^{*†}

School of Materials Science and Engineering, Woodruff School of Mechanical Engineering, Georgia Institute of Technology, Atlanta, Georgia 30332

Received April 15, 2010; E-mail: yushin@gatech.edu

The use of Li-alloy anodes offers great potential for increasing the specific capacity of Li-ion battery anodes and thus lowering battery weight and volume.^{1–4} Particular attention has been given to Si–Li alloys due to their high theoretical capacity.^{1,4–6} The large volume change in the anode alloy during Li insertion and extraction may lead to electrode failure.⁷ However, the use of porous anodes with voids capable of accommodating these volume changes^{6,8} may allow for stable battery operation.

The stability of the interface between the electrically conductive C particles and the significantly less conductive Si particles in a composite anode is often critical for maintaining the conductivity of the anode during charge–discharge cycling.⁶ This interface may be broken if its endurance limit is exceeded by the amplitude of the interface stresses. The stresses during cycling are related to the current rate and both the material properties (such as the equilibrium volume changes in Si and C upon Li insertion/extraction) and the sample geometry (such as the curvature of the interface, the thickness of the Si or C layers, and the dimensions of the continuous interface, among others). Earlier work on Si thin films deposited on Cu or Ni foils revealed several important observations. First, decreasing the Si film thickness significantly enhances its stability.⁹ Second, even relatively thin films deposited on flat Cu foil become cracked after cycling.¹⁰ Nonetheless, crack formation may not necessarily prevent stable anode performance.¹⁰ If one deviates from flat sample geometry, and if Cu is replaced with C, one may expect significant differences in the behavior of the Si anode. Due to fewer dangling bonds on the C surface, the Si–C interface strength may be significantly reduced. Gaining a better fundamental understanding of the possible changes in nano-Si morphology during cycling is also needed for achieving robust battery operation. Apart from the structural stability of the anode, designing a stable solid-electrolyte interface (SEI) may be critically dependent on such knowledge. Yet, it is still largely unclear to the community if the pores in a structured Si anode will change size or collapse during long-term battery operation, and under what conditions the Si anode nanoparticles may resume their original shape after extraction of Li from the lithiated phase.

Here we report a simple model of Si deformation upon electrochemical alloying and dealloying with Li in a nano confined space and apply it for a Si film deposited on and weakly bound to the inner surface of a size-preserving tubular material. To verify this model, we utilize carbon nanotubes (CNTs) with an inner Si coating and report a systematic experimental study on the effect of the Si film thickness on the particles' microstructural changes and electrochemical performance.

The computational model of an elastoplastic ring inside a circular constraint (see the Supporting Information, SI) assumes the volume

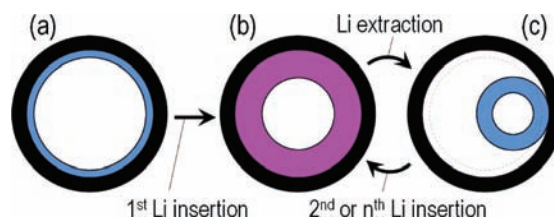


Figure 1. Results of the computational modeling of shape changes of a Si tube inside a rigid nanopore during reaction with Li.

changes in long Si–Li tubes to be accommodated solely by the wall thickness so that the tube length remains unchanged. The results of this model are shown in Figure 1.

The Li-alloying material (e.g., Si) tube is initially attached to the pore walls (Figure 1a). During insertion of Li, the rigid matrix restricts the inner tube's outer expansion, forcing the Si–Li alloy material to expand inward and decrease the cylinder's internal diameter (Figure 1b). This inward expansion is accompanied by plastic deformation. The rigid outer matrix, however, does not prevent a reduction of the tube's outer diameter when Li is extracted (Figure 1c), if the bonding between the Si–Li alloy and the outer surface is weak. Upon Li extraction, the tube does not restore its initial geometry but rather tightens to a smaller size. As a result of this contraction, the inner tube separates from the matrix wall, except at a specific spot (Figure 1c), at which the bonding is somewhat stronger. During consecutive Li insertions, the separated tube can expand outward until its outer diameter matches the pore size. In other words, sequential Li insertion and extraction periodically alters the tube size between the expanded and contracted states (Figure 1b and 1c), whereas the first Li insertion modifies the initial shape to match the pore size in the expanded state.

To experimentally verify the model's predictions, alumina membranes with ~300 nm pores were subsequently coated with (a) ~40 nm of C *via* C₃H₆ decomposition at 700 °C at atm pressure, (b) Si of various thicknesses *via* SiH₄ decomposition at 500 °C, and (c) ~5 nm of C and etched in a HF solution. The synthesized membranes, consisting of nearly identical vertical tubes (Figure 2a), were mechanically and electrically connected to the Cu foil current collector using a PVDF binder (Figure 2b). The samples were tested in 2016 coin cells with a Li metal counter electrode at the rate of ~C/20. Selected samples were tested at C/1 to evaluate cycling stability.

Transmission electron microscopy (TEM) of all but the 9 wt % Si samples showed the evident contraction and partial delamination of the inner Si tube from the CNT surface after the Li extraction (Figures 2c,d). Similar levels of Si inner tube contraction were observed after the 1st and the 10th cycles, suggesting reversible shape changes in those Si particles having no external restrictions.

While pure Si behaves as a very brittle material during mechanical deformations at room temperature, it is evidently capable of

[†] School of Materials Science and Engineering.

[‡] School of Mechanical Engineering.

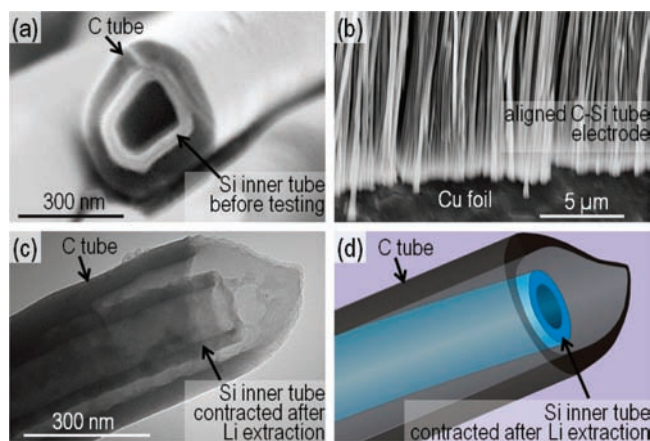


Figure 2. Electron microscopy of the composite Si-in-C tubes: (a) scanning electron microscopy (SEM) of one of the synthesized samples, (b) SEM of the electrode attached to a Cu current collector, (c) TEM and (d) its schematic of the sample after Li extraction at the 10th cycle.

adapting to the restricted shape of the pore and plastically deforming during reversible electrochemical alloying with Li. This finding may explain the somewhat counterintuitive observations that rigid binders are efficient for Si powder electrodes,^{8,11,12} in spite of the particles' large volume changes during cycling. The degree of Si tube contraction increased with increasing Si thickness, as qualitatively predicted by the model. We did not observe any increase in Si tube length after cycling. The compressed Si tubes were typically attached to one of the CNT walls, providing electrical contact. Multiple cracks previously seen in planar thin Si films¹⁰ were not observed in tubular samples. No major defects in the carbon walls were observed after cycling.

The capacity of the samples was close to theoretical capacity only for the 9 wt % Si sample, which did not show evident delamination, or for the 33 and 46 wt % Si samples (Figure 3a). We hypothesize that sufficiently thin Si tubes delaminated from the CNT became partially electrically isolated during cycling. Interestingly, the composite samples with a Si content of 46 wt % showed a capacity of 2100 mAh/g, very close to the theoretical maximum predicted, assuming Si's contribution to be 4200 mAh/g (Figure 3a). This is consistent with observations on other nano-Si materials^{13,14} and is higher than what was observed for micro-Si.¹⁵ The volumetric capacity of the 46 wt % sample was as high as 1505 mAh/cc. Further optimization of Si and C wall thickness may further increase the capacity.

The samples produced showed moderate rate capability, but excellent stability (Figure 3b), as expected from the model (Figure 1). The porous composite particles require little (<3 wt %) binder, in contrast to Si nanopowder, which often demands as high as 33 wt % binder for a stable electrochemical performance.⁸

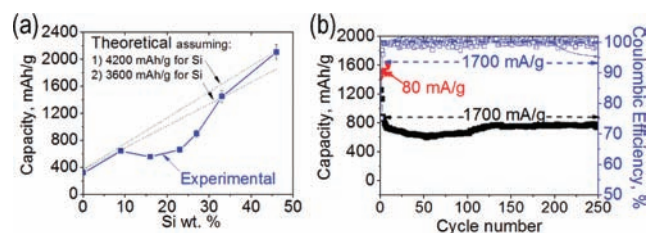


Figure 3. Electrochemical performance of the composite Si-in-C tubes in half cells: (a) deintercalation capacity at the first cycle after an SEI formation recorded at the C/20 rate as a function of Si content; (b) deintercalation capacity retention and Coulombic efficiency for the sample containing 33 wt % Si. The reported capacity is normalized by the total weight of C and Si.

Another key advantage of the size-preserving external rigid carbon shell is the very high value of the Coulombic efficiency (CE) achievable in such samples. Note that the loss of even 1% of the cell's Li due to electrolyte decomposition in each cycle (CE = 99%) would lead to nearly complete degradation of the balanced full cell after 100 cycles. The minimal volume changes of graphitic anodes during operation allow them to form a stable SEI layer impermeable to solvent molecules, which serves as a barrier to electrolyte decomposition and leads to a CE > 99.9% after the first cycle. In comparison, the dramatic volume changes in Si during electrochemical alloying and dealloying with Li prevent the formation of a stable SEI layer. Si nanowires with and without C coating demonstrate a CE of 93–98%,^{1,16,17} and Si nanoparticles bridged and coated with a binder and/or C show a CE of 93–99%.^{6,12,18,19} In contrast, our samples demonstrate an average CE of 99.6% for cycles 2–50 and in excess of 99.9% for cycles 50–250 (Figure 3b). The CE of 75% at the first cycle can likely be improved with C surface modification.²⁰

In summary, we have proposed a simple model to predict shape changes in Si upon electrochemical reaction with Li in a nano-confined geometry. Our experiments confirmed our theoretical predictions and demonstrated irreversible shape changes in the first cycle and fully reversible shape changes in subsequent cycles. The produced porous Si with a rigid C outer shell showed high capacity, stable performance, and outstanding CE. The CNT walls were demonstrated to be capable of withstanding stresses caused by the initial Si expansion and Li intercalation. These findings provide guidance for the efficient design of building blocks for viable nano-Si anodes.

Acknowledgment. We thank NASA and NSF for partial financial support as well as A. Magasinski and Y. Ding for TEM assistance.

Supporting Information Available: Additional details for modeling, sample fabrication, and characterization. This material is available free of charge via the Internet at <http://pubs.acs.org>.

References

- Chan, C. K.; Peng, H. L.; Liu, G.; McIlwrath, K.; Zhang, X. F.; Huggins, R. A.; Cui, Y. *Nat. Nanotechnol.* **2008**, *3*, 31.
- Poizot, P.; Laruelle, S.; Grugeon, S.; Dupont, L.; Tarascon, J. M. *Nature* **2000**, *407*, 496.
- Taberna, L.; Mitra, S.; Poizot, P.; Simon, P.; Tarascon, J. M. *Nat. Mater.* **2006**, *5*, 567.
- Oumellal, Y.; Rougier, A.; Nazri, G. A.; Tarascon, J. M.; Aymard, L. *Nat. Mater.* **2008**, *7*, 916.
- Poizot, P.; Laruelle, S.; Grugeon, S.; Dupont, L.; Tarascon, J. M. *J. Power Sources* **2001**, *97–8*, 235.
- Magasinski, A.; Dixon, P.; Hertzberg, B.; Kvit, A.; Ayala, J.; Yushin, G. *Nat. Mater.* **2010**, *9* (4), 353–358.
- Huggins, R. A. *J. Power Sources* **1999**, *81*, 13.
- Beattie, J. S. D.; Larcher, D.; Morcrette, M.; Simon, B.; Tarascon, J. M. *J. Electrochem. Soc.* **2008**, *155*, A158.
- Takamura, T.; Ohara, S.; Uehara, M.; Suzuki, J.; Sekine, K. *J. Power Sources* **2004**, *129*, 96.
- Maranchi, J. P.; Hepp, A. F.; Kumta, P. N. *Electrochem. Solid-State Lett.* **2003**, *6*, A198.
- Li, J.; Lewis, R. B.; Dahn, J. R. *Electrochem. Solid-State Lett.* **2007**, *10*, A17.
- Magasinski, A.; Zdyrko, B.; Kovalenko, I.; Hertzberg, B.; Burtovyy, I.; Fuller, T.; Luzinov, I.; Yushin, G. Submitted.
- Bridel, J. S.; Azais, T.; Morcrette, M.; Tarascon, J. M.; Larcher, D. *Chem. Mater.* **2010**, *22*, 1229.
- Kang, K.; Lee, H. S.; Han, D. W.; Kim, G. S.; Lee, D.; Lee, G.; Kang, Y. M.; Jo, M. H. *Appl. Phys. Lett.* **2010**, *96*, 053110.
- Obrovac, M. N.; Christensen, L. *Electrochem. Solid-State Lett.* **2004**, *7*, A93.
- Chan, C. K.; Ruffo, R.; Hong, S. S.; Huggins, R. A.; Cui, Y. *J. Power Sources* **2009**, *34*.
- Kim, H.; Cho, J. *Nano Lett.* **2008**, *8*, 3688.
- Mazouzi, D.; Lestriez, B.; Roue, L.; Guyomard, D. *Electrochem. Solid-State Lett.* **2009**, *12*, A215.
- Chou, S. L.; Wang, J. Z.; Choucair, M.; Liu, H. K.; Stride, J. A.; Dou, S. X. *Electrochem. Commun.* **2010**, *12*, 303.
- Aurbach, D. *J. Power Sources* **2000**, *89*, 206.

JA1031997